Turkish Journal of Electrical Engineering and Computer Sciences

Volume 23 | Number 4 Article 17

1-1-2015

# Impact of repeaters on the performance of indoor visible light communications

REFİK ÇAĞLAR KIZILIRMAK

Turkish Journal of Electrical Engineering & Computer Sciences

http://journals.tubitak.gov.tr/elektrik/

Research Article

Turk J Elec Eng & Comp Sci
(2015) 23: 1159 – 1172

doi:10.3906/elk-1212-22

# Impact of repeaters on the performance of indoor visible light communications

**Refik Çağlar KIZILIRMAK***
Department of Electrical and Electronics Engineering, KTO Karatay University, Konya, Turkey

**Received:** 04.12.2012 • **Accepted/Published Online:** 01.08.2013 • **Printed:** 10.06.2015

**Abstract:** In this study, we examine the performance of fixed gain amplify-and-forward repeaters for visible light communication (VLC) systems. We present the wireless optical channel model for VLC with the repeater and we evaluate the bit-error-rate (BER) performance for pulse-position modulation over the multipath channel with additive white Gaussian noise. The results reveal that when a repeater is placed, both the BER and the illuminance performance can be improved at any location in a typical office space. The benefit of VLC repeaters is also discussed when the channel from the source to the destination is shadowed. It is found that when the channel is shadowed, the impact of repeaters on the communication reliability is more distinct.

**Key words:** Visible light communications, pulse position modulation, repeater, shadowing

## 1. Introduction

In recent years, visible light communication (VLC) has emerged as a new wireless communication technology and it is expected to find places in many wireless communication applications, such as inter-/intravehicle communication, hospitals and health care services, hazardous environments, defense and security services, aviation, and underwater communications [1][2][3]. The VLC technology relies on the intensity modulation and direct detection for data transmission (IM/DD). The majority of the existing works focused on utilizing LEDs at the transmitter to emit the intensity and a photodiode (PD) at the receiver to detect the received intensity.

There are a number of constraints on designing a VLC system. First of all, the main role of such systems is to illuminate the location at which they have been installed. Any flickering or color shift in the light is not acceptable, which can occur depending on the modulation scheme [4]. There are other constraints for designers such as full brightness of the source, protection of the human eye, and dimming-control ability. An on-off keying (OOK) modulation scheme is commonly used in the literature for VLC [5]. In OOK, it is possible to achieve full brightness and dimming control; however, color shifts and flickering can appear without coding [6]. Pulse-position modulation (PPM) is another commonly used modulation scheme in which the same power is consumed to transmit the different symbols, which provides flicker-free emission. It is also possible to achieve full brightness with PPM. However, it is difficult to control the brightness of LED lighting by OOK.

In addition to its illumination role, a VLC system should convey information from the source to the destination. In a typical VLC communication link, there is a number of source terminals, each consisting of LED chips, and there is no intermediate terminal between the source and the destination. In this work, we consider

*Correspondence: refik.kizilirmak@karatay.edu.tr

a single intermediate station in an indoor VLC channel as a repeater in order to improve the reliability and the illuminance performance of the system. There are some works in the literature that considered intermediate stations for wireless optical communication: in [7][8][9], intermediate stations are placed as relays to provide multihop diversity to the destination for free-space optical (FSO) communication. FSO communication links experience multipath and fading effects over long distances. Since the indoor VLC channels are not expected to fade and they are usually modeled as AWGN channels, the diversity techniques are not the subject for such channels [10]. There are also some hybrid models proposed in the literature considering intermediate terminals. In [11], a desktop lamp was demonstrated as an intermediate terminal that receives a radio signal and repeats it to the desk over the visible light channel. Similarly, in [12], an intermediate terminal receives information from a power-line communication (PLC) channel and then retransmits it through a visible light channel.

In radio communication, repeaters are commonly used in order to extend the coverage performance of the network. Repeater-assisted networks are different from relay-assisted networks. In relay-assisted networks, intermediate stations relay the information to the destination in order to provide different replicas of the same information, which are then combined using a combining circuit [13]. The main difference between repeating and relaying is that the relay stations do not listen and transmit at the same time but use additional scheduling algorithms such as TDMA, FDMA, CDMA, etc. On the other hand, repeaters do not need any additional scheduling algorithm and can be employed in any existing network without any prior work. One of the disadvantages of the repeaters is that they introduce interference to the network caused by the delay added to the signal at the repeater circuit.

The VLC links can also be shadowed or blocked by moving objects in the environment. In [14], the chance of shadowing for VLC channels is driven according to the room geometry and human obstruction probability. It is not easy to draw a general model and accurately calculate the probability of shadowing; such chance is given as less than 2% in a typical office with 3-m ceiling height. In [15], the effect of shadowing was investigated according to the obstacles' traffic density in the channel and installing spatially distributed multiple sources was proposed to combat shadowing. One of the main drawbacks of using multiple sources is that driving all the LED chips synchronously is a difficult task and requires a careful design of the cable lengths and the spacing between LED chips [16].

In this work, we consider a single intermediate station mounted on the desk in an indoor VLC channel as a repeater in order to improve the reliability and the illuminance performance of the system. In the considered system, all the transmission between the terminals occur in the visible light medium at the same frequency band. We consider binary-PPM, which is a standard modulation scheme for wireless optical communications. Intersymbol interference (ISI) due to the propagation delay and the delay added by the repeater is also discussed as a data rate limiting factor. In this work, we limit our study to the case in which there is no ISI present in the channel.

The remainder of the paper is as follows: Section 2 presents the wireless optical channel model. Section 3 discusses the transmission scheme and the receiver structure. Section 4 gives the numerical results including the optimum repeater height, bit-error-rate (BER), and illuminance performance improvement with the repeater. The impact of repeaters in a shadowed communication channel is also discussed in this section. Section 5 concludes the paper.

## 2. Wireless optical channel model

In order to emphasize the practical usage of repeaters for VLC, we have considered an empty room model as the physical environment. The room is $5 \times 5 \times 3$ m, and the optical source is installed at the center of the ceiling. The main purpose of the optical source is to illuminate a desk surface. In our model, the performance of the system is evaluated at the desktop height of 0.85 m. Throughout the paper, the model without any intermediate terminal is taken as the reference model that is to be compared with the repeater-assisted model. Figure 1 illustrates the reference channel and the repeater-assisted channel models.

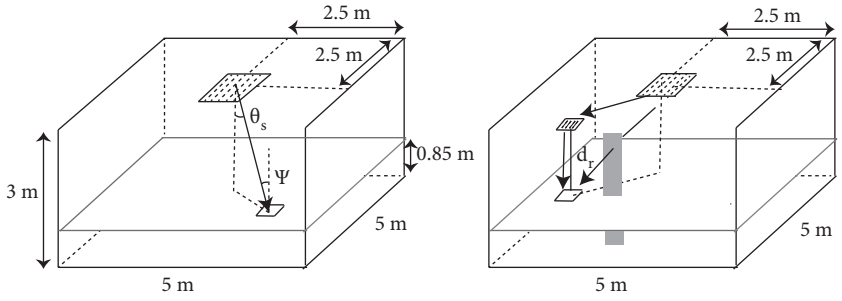


**Figure 1**. (a) Reference channel model, (b) repeater-assisted channel model with possible shadowing.

### 2.1. Reference channel model

In a typical short-range VLC link, the electro-optical conversion is performed by an LED at the transmitter, and a silicon photodiode performs direct detection of the incident optical intensity at the receiver. The received photocurrent $y(t)$ is given by [17]:

$$y(t) = rI(t) * h(t) + n(t), \tag{1}$$

where $r$ is the responsivity $(A/W)$, $I(t)$ is the transmitted intensity, $n(t)$ is the noise, $h(t)$ is the channel response, and $*$ denotes the convolution operation. The electro-optical conversion can be considered as linear so that $I(t) = gx(t)$ where $g$ is the gain of the device in unit of $W/A$ and $x(t)$ is the electrical current signal that is the information source. Hence, Eq. (1) can be rewritten as:

$$y(t) = rgx(t) * h(t) + n(t). \tag{2}$$

Note that $x(t)$ must be nonnegative and the average intensity of all emissions $\lim_{T\to\infty} \frac{1}{2T} \int_{-T}^{T} gx(t)dt$ is also limited due to eye safety regulations.

The noise at the receiver consists of the ambient shot noise in the photodiode and the thermal noise. The shot noise in the photodiode can accurately be modeled as white Gaussian and independent of $x(t)$. The thermal noise at the receiver is also Gaussian. Therefore, the VLC channel noise $n(t)$ is assumed to be an additive white Gaussian (AWGN) noise [18].

The VLC channel $h(t)$, as for other wireless optical channels, consists of line-of-sight (LOS) and diffuse or non-line-of-sight (NLOS) components:

$$h(t) = h_{LOS}(t) + h_{diff}(t). \tag{3}$$

The LOS part of the channel can be modeled by delayed Dirac pulses as

$$h_{LOS}(t) = g_{LOS}\delta(t - \Delta t_{LOS}), \tag{4}$$

where $g_{LOS}$ and $\Delta t_{LOS}$ are the gain and the delay of the LOS components. When all the LED chips are perfectly synchronized at the source terminal, $\Delta t_{LOS}$ becomes ideally zero. In [16], with the detailed cabling design, all the LOS components from each LED chip arrive at the receiver within $\Delta t_{LOS} = 5$ ns. The diffuse portion comes from the reflections of the room's objects and walls. Experimental measurements [19] and ray-tracing simulations [20] have been used to estimate the diffused channel. In [21], the diffused channel was analytically modeled (integrating-sphere model) as

$$H_{diff}(f) = g_{diff}\frac{\exp(-j2\pi f\Delta t_{diff})}{1 + jf/f_0}, \tag{5}$$

where $g_{diff}$ and $\Delta t_{diff}$ are the gain and the delay of the diffuse component and $f_0$ is the 3-dB cut-off frequency of a diffuse channel.

The channel response including LOS and NLOS components becomes

$$H(f) = g_{LOS}\exp(-j2\pi f\Delta t_{LOS}) + g_{diff}\frac{\exp(-j2\pi f\Delta t_{diff})}{1 + jf/f_0}. \tag{6}$$

The VLC channel DC gain $H(0)$ then becomes $g_{LOS} + g_{diff}$. The channel gains are given in [16] as

$$g_{LOS} = A_R(m_L + 1)\frac{\cos^{m_L}(\theta)\cos(\psi)}{2\pi d^2}, \tag{7}$$

$$g_{diff} = \frac{A_R\sin^2(\mathrm{FOV})\rho}{A_{room}(1 - \rho)}, \tag{8}$$

where $m_L$ is the order of Lambertian emission, $A_R$ is the physical area of the receiver, $A_{room}$ is the room area, FOV is the field of view of the detector, $\rho$ is the average reflectivity from the walls, $\theta$ and $\psi$ are the angles of irradiance and incidence, and $d$ is the distance between the transmitter and the receiver as shown in Figure 1a. According to the used model in Eq. (8), the gain of the diffuse portion $g_{diff}$ is the same at every location in the room [16]. The order of Lambertian emission $m_L$ is given in [18] as

$$m_L = -\frac{\ln 2}{\ln(\cos\Phi_{1/2})}, \tag{9}$$

where $\Phi_{1/2}$ is the LED semiangle at half power.

The average received optical power $P_r$ is the product of the transmission power and channel DC gain [22]:

$$P_r = H(0)P_t. \tag{10}$$

$H(0)$ can be increased by narrowing $\Phi_{1/2}$. The LOS component considerably dominates the channel response in most cases. In [23], the multipath channel profiles for the VLC and infraRed (IR) channels were compared. It was reported that the magnitude of the reflected path for the VLC channel is smaller than that for the IR channel.

The signal-to-noise ratio (SNR) is defined as the ratio of total electrical power generated by the photodiode to the noise power:

$$\text{SNR} = 2r^2 P_r^2 / N_0 B, \tag{11}$$

where $N_0$ is the double-sided power spectral density of the noise, $P_r$ is the received optical power as calculated in Eq. (10), and $r$ is the responsivity. If the data rate for 2-PPM is $R_b$, then the equivalent noise bandwidth $B$ is $2R_b$. The noise term includes the shot noise and the thermal noise:

$$N_0 = N_{shot} + N_{thermal}. \tag{12}$$

The thermal noise is usually constant and depends on the temperature, but shot noise is related to the amount of light incident on the photodetector. The mean-squared noise current from the photodetector is $qI_{bg}$. The shot noise density is then as given in [16]:

$$N_{shot} = qI_{bg} \quad \text{A}^2/\text{Hz}, \tag{13}$$

where $q$ is electron charge ($1.6 \times 10^{-19}$ C) and $I_{bg}$ is the background light induced current. For example, $I_{bg}$ of 5.1 mA [24] will generate a shot noise power of $8.1 \times 10^{-16}$ mW/Hz (-150.9 dBm/Hz). For many applications, thermal noise is smaller than the ambient light noise and can be neglected, $N_0 \simeq N_{shot}$ [16].

A wireless optical channel can be seen as a low-pass electrical channel. A white-light LED can usually provide 2 MHz of modulation bandwidth [17] and the 3-dB cut-off frequency of the channel is described as $H(f_{3dB}) = 0.707H(0)$.

Using Eq. (6), with average $\Delta t_{LOS} = 2$ ns and considering that the channel bandwidth is dominated by the LOS component, the approximate channel bandwidth $f_{3dB}$ becomes 90 MHz. In this case, the transmission bandwidth $B$ becomes limited by 2 MHz, which is the modulation bandwidth of the white-light LED. When binary-PPM is considered, the bandwidth efficiency is 1/2 and the achievable data rate $R_b$ becomes 1 Mbps. The transmission at 1 Mbps is ISI-free transmission since the time dispersion in the channel is on the order of nanoseconds.

Finally, the illuminance is defined as the total luminous flux incident on an illuminated surface. The illuminance $E$ at a point on the surface is given by [24]

$$E = \frac{I_v(0) cos^m(\theta)}{d^2} cos(\psi), \tag{14}$$

where $I_v(0)$ is the center luminous intensity.

### 2.2. Repeater-assisted channel model

In our repeater-assisted channel model, we place a repeater (or use an existing desk LED lamp) on the desk at the height of $\text{d}_r$ and tilt it down to the desk surface, as in Figure 1b. A possible blocking body is also indicated in Figure 1b.

The total number of LED chips used in the repeater-assisted model is kept the same as in the reference channel model. The source emits the information with no awareness of the intermediate repeater in the environment. The repeater receives the emitted signal by its PD, converts it to an electrical signal, and amplifies and emits the information by its LEDs.

If the optical power of the source terminal is $P_s$, then the received photocurrent $y_r(t)$ by the repeater becomes

$$y_r(t) = rP_sI(t)*h_{sr}(t) + n_r(t), \tag{15}$$

where $h_{sr}(t)$ is the channel response between the source and the repeater, and $n_r(t)$ is the additive noise term at the repeater. The repeater amplifies the noisy signal and emits it back to the destination. The choice of the amplification gain $G$ in terms of the ratio of the output electrical power to the input electrical power, assuming $rg = 1$ for the repeater terminal, is [25]:

$$G = \frac{P_r^2}{(P_sH_{sr}(0))^2 + N_0/2}, \tag{16}$$

where $P_r$ is the optical power of the repeater. The gain in Eq. (16) does not depend on the instantaneous channel state information (CSI) and hence it is fixed.

The received photocurrent $y_d(t)$ at the destination then becomes

$$y_d(t) = r[\sqrt{G}(P_srI(t)*h_{sr}(t) + n_r(t))*h_{rd}(t) + P_sI(t)*h_{sd}(t)] + n_d(t), \tag{17}$$

where $h_{sr}(t)$ and $h_{rd}(t)$ are the channel responses for the links of the source-repeater and the repeater-source, respectively, and $n_d(t)$ is the noise added at the destination.

## 3. Transmission model

We consider pulse position modulation (PPM) for the transmission, which is a standard modulation technique used in optical communications. Figure 2 displays the block diagram of the $M$-PPM ($M$ is the modulation order) transmission through a repeater. In $M$-PPM, an optical pulse is transmitted in one of the nonoverlapping $M$ time slots per symbol. The structure of the source terminal is given in Figure 2a. The bit sequence $a_k$ at a rate of $\log_2 M/T$ is fed into the block encoder where $T$ is the duration of the PPM symbol. The block coder produces a symbol vector of length $M$ in which one chip has $\log_2 M$ bits of information and $M-1$ chips carry zero chip values. Parallel-to-series conversion then converts the vector into a chip sequence $b_k$ at a rate of $M/T$. The chip sequence is scaled to the optical power $P_s$, which is followed by the transmitter pulse shape $p(t)$. The transmitter pulse is of a rectangular shape with unit magnitude and duration of $T/M$. A basis set for $M$-PPM, $\phi_m(t)$ for $m \in \{1,2,\ldots,M\}$ is

$$\phi_m(t) = p\left(t - \frac{T}{M}(m-1)\right). \tag{18}$$

A time-domain representation of the intensity waveform as sent from the source terminal is

$$I(t) = \sum_{k=-\infty}^{\infty} \phi_{b_k}(t - kT)g. \tag{19}$$

The signal reaches the repeater over the multipath channel. The noisy signal is amplified at the repeater by $G$ to the optical power level of $P_r$ and then emitted by its LEDs as shown in Figure 2b.

The photodetector at the receiver receives signals from both the source and the repeater. A matched filter $g(t) = \sqrt{M/T}p(T-t)$ is employed at the receiver with unit energy. The sampler performs at the chip rate

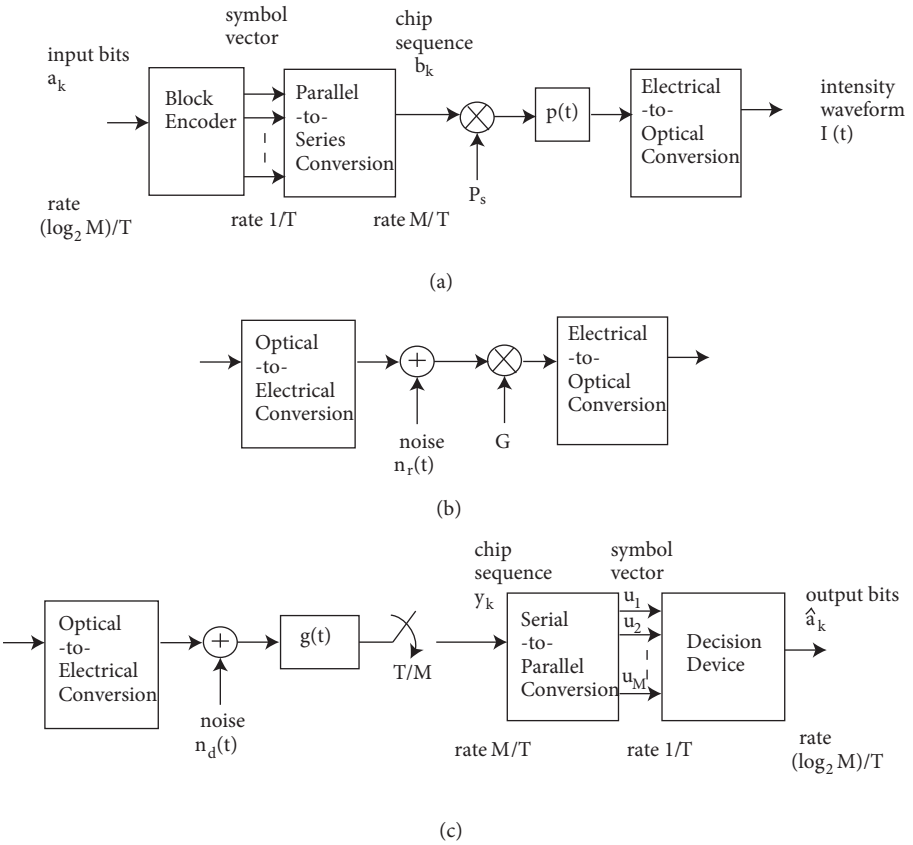


**Figure 2**. Simplified block diagram of the transmission model: (a) source terminal, (b) repeater terminal, (c) receiver.

of $T/M$. The receiver makes its decision based on the largest element of the received vector $\mathbf{u} = [u_1 u_2 \dots u_M]$. The decision variables to be fed into the detector at the output of the matched filter, assuming that the $k$th chip conveys the information, are

$$u_k = rP_s[H_{sd}(0) + \sqrt{G}H_{rd}(0)H_{sr}(0)] + [\sqrt{G}H_{rd}(0)n_r + n_d], \tag{20}$$

$$u_\ell = \sqrt{G}H_{rd}(0)n_r + n_d, \tag{21}$$

where $\ell, k \in \{1,2,\dots,M\}$ and $\ell \neq k$, $P_s$ is the optical power for each symbol emitted by the source under full brightness, $H_{sr}(0)$ and $H_{rd}(0)$ are the channel DC gains for the source-repeater and repeater-destination links, and $n_r$ and $n_d$ are the additive noises at the repeater and the destination nodes that are independent of each other with variances $N_0/2$. The BER for 2-PPM transmission with the repeater then becomes [10]

$$P_e = Q\left(\frac{rP_s(H_{sd}(0) + \sqrt{G}H_{rd}(0)H_{sr}(0))}{\sqrt{N_0/2(GH_{rd}(0)^2 + 1)}}\right). \tag{22}$$

Indoor wireless optical links can be a subject of shadowing generally caused by standing people in the environment. When the source-destination link is shadowed, the communication will continue over the diffused path of that link. If the probability of blocking the LOS path of the source-destination link is $P_{block}$, Eq. (22)

can be modified as

$$P_e = Q\left(\frac{rP_s(H_{sd}(0)+\sqrt{G}H_{rd}(0)H_{sr}(0))}{\sqrt{N_0/2(GH_{rd}(0)^2+1)}}\right)(1-P_{block}) + Q\left(\frac{rP_s(g_{diff}+\sqrt{G}H_{rd}(0)H_{sr}(0))}{\sqrt{N_0/2(GH_{rd}(0)^2+1)}}\right)(P_{block}). \quad (23)$$

The receiver structure in Figure 2c is designed to perform in the absence of ISI. The received optical signal experiences time dispersion due to the reflections from walls and other surrounding materials. In the measurements for VLC in [23], all the rays from LOS and NLOS paths arrive at the destination in less than 20 ns in an indoor environment and it heavily depends on the room geometry and the wall materials. The repeater circuit also inserts a delay, which causes wider time dispersion in the channel than the reference channel model. The time dispersion in the channel due to the diffused and repeated paths gives rise to ISI, which reduces either the reliability or the rate of the transmission. In the literature, a number of techniques have been proposed to combat ISI for indoor wireless optical channels. In [26], a guard interval was inserted in each symbol frame with a cost of throughput. In [27], spread spectrum techniques were considered; however, they decreased the bandwidth efficiency. In [28] an angle diversity scheme with multibeam narrow FOV transceiver was proposed, which spatially exploited the time-dispersed channel components. In [29] an adaptive equalizer was employed to mitigate the effects of ISI.

In $M$-PPM transmission, ISI occurs when all the paths from the source and the repeater arrive at the destination within a duration of longer than $T/M$ s. The latest path propagates through the diffused path of the source-repeater link, then is amplified and reaches the destination through the diffused path of the repeater-destination link, which makes the total propagation time of $2\tau_p + \tau_r$ s where $\tau_p$ and $\tau_r$ are the propagation delay and the delay added by the repeater, respectively. Therefore, the maximum achievable ISI-free data rate with the repeater channel becomes $\frac{1}{M(2\tau_p+\tau_r)}$ sym/s.

In [30], a simple and fast photodiode amplifier circuit was given. The propagation delay $\tau_r$ for the circuitry was given as 45 ns, which causes wider time dispersion in the channel as compared to the reference channel. In this case, the channel bandwidth depends on the power allocation between the source and repeater terminals and also their distances to the destination terminal. With the described configuration in the Table and $d_r = 0.7$ m, the 3-dB channel bandwidth distribution in the room area is given in Figure 3. Only the upper right corner of the room area is presented due to the symmetry. The minimum 3-dB channel bandwidth of the channel with the repeater is 3.42 MHz. Therefore, for the repeater-assisted channel, the transmission bandwidth is again limited to the modulation bandwidth of the LED chips, which is 2 MHz. The maximum achievable data rate for 2-PPM becomes 1 Mbps. The transmission at this rate will not experience ISI since half of the symbol duration of 0.5 $\mu$s is much larger than $2(2\tau_p + \tau_r)$, which is on the order of nanoseconds.

## 4. Results and discussion

The performance improvement with the repeater has been evaluated through analytical calculations and computer simulation. The transmission rate $R_b$ is taken as 1 Mbps for both reference and repeater-assisted channel models. The Table gives the parameters considered in the evaluations. The total number of LEDs were kept the same in both the reference channel and the channel with the repeater for a fair comparison. The number of LED chips and the total luminous intensity for a desk lamp are consistent with the previous research in the literature. In [12], a table lamp was used as a source of VLC communication with 120 LED chips, each having luminous intensity of 1.56 cd.

**Table.** System component parameters.

| | |
|---|---|
| Semiangle half power ($\Phi_{1/2}$) | $120^o$ |
| Center luminous intensity of an LED chip ($I_v(0)$) | 1.56 cd |
| Number of LEDs in the reference model | 1200 |
| Number of LEDs in the repeater model | 120/1080 |
| FOV at a receiver (FOV) | $60^o$ |
| Detector physical area ($A_r$) | 1 $cm^2$ |
| Detector responsivity ($r$) | 0.53 A/W |
| Data rate ($R_b$) | 1 Mbps |
| LED chip optical power | 4 mW |
| Signal bandwidth ($B$) | 2 MHz |
| Noise density ($N_0$) | -150.9 dBm/Hz |
| Average reflectivity ($\rho$) | 0.2 |

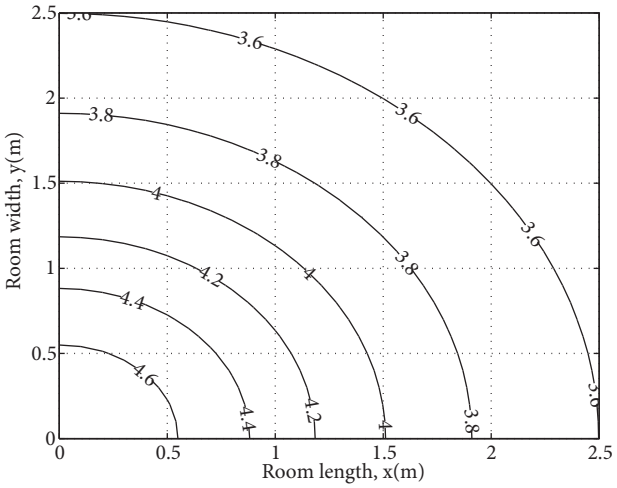


**Figure 3**. 3-dB channel bandwidth (MHz) distribution for the repeater-assisted channel: min. 3.42 MHz, mean 3.86 MHz, max. 4.75 MHz.

### 4.1. Effect of the repeater height

Figure 4 gives the relationship with the SNR improvement and the illuminance for different repeater heights $d_r$. The computer simulation was run for every 0.01 $m^2$ in a 5 $\times$ 5 $m^2$ room at the desk height of 0.85 m. We define the SNR improvement in terms of SNR gain achieved by the repeater with respect to the reference channel when BER = $10^{-3}$ for both cases. The channel gain $H_{sd}(0)$ is set to unity. For each location of the receiver, the DC gains of the channels $H_{sr}(0)$ and $H_{rd}(0)$ with their LOS and NLOS components are then normalized to the channel gain between the source and the destination $H_{sd}(0)$. The SNR improvement values are averaged over each repeater location.

The illuminance is calculated by Eq. (14) for every 0.01 $m^2$ in the room and the minimum level is considered in order to achieve adequate brightness. In EN 12464-1, 400 lx is given as the minimum brightness required for a work place. When $d_r$ is less than 70 cm, the required brightness is achieved at every location in the room. When $d_r$ is 70 cm, the average SNR improvement is 2.78 dB and the minimum illuminance at the desk surface is 408 lx. In the rest of the analysis, the repeater is placed at 70 cm in height from the desk surface.

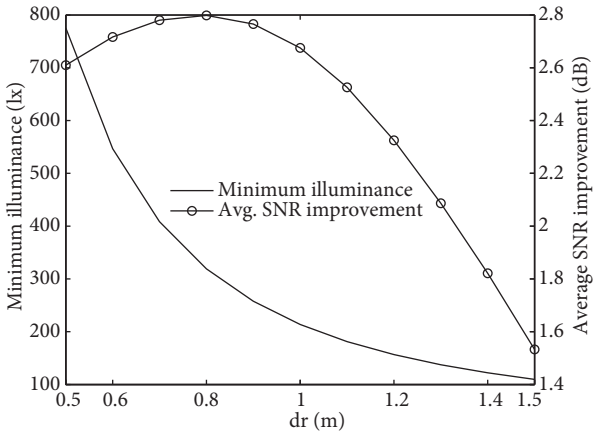


**Figure 4**. SNR improvement and illuminance for different $d_r$ values.

### 4.2. Illuminance distribution

Figure 5 compares the distributions of the illuminance at the desk surface for the reference channel and repeater-assisted channel. Due to the symmetry of the room geometry, only the upper right corner of the room area is considered in the simulation. Figure 5a gives the distribution of the illuminance for the reference model. In the reference channel model, with 1200 LED chips (each having center luminous intensity of 1.56 cd), it cannot achieve the target illuminance of 400 lx at the desk surface. When a repeater with 120 LED chips is installed at the desk and the remaining 1080 LED chips are used for the source at the ceiling, the illuminance at the desk surface is dramatically increased. The illuminance distribution with the repeater can be found in Figure 5b. On average, with the described allocation ratio of LED chips, a desk lamp increases the average illuminance 3.49 times at the desk surface with respect to the reference model.

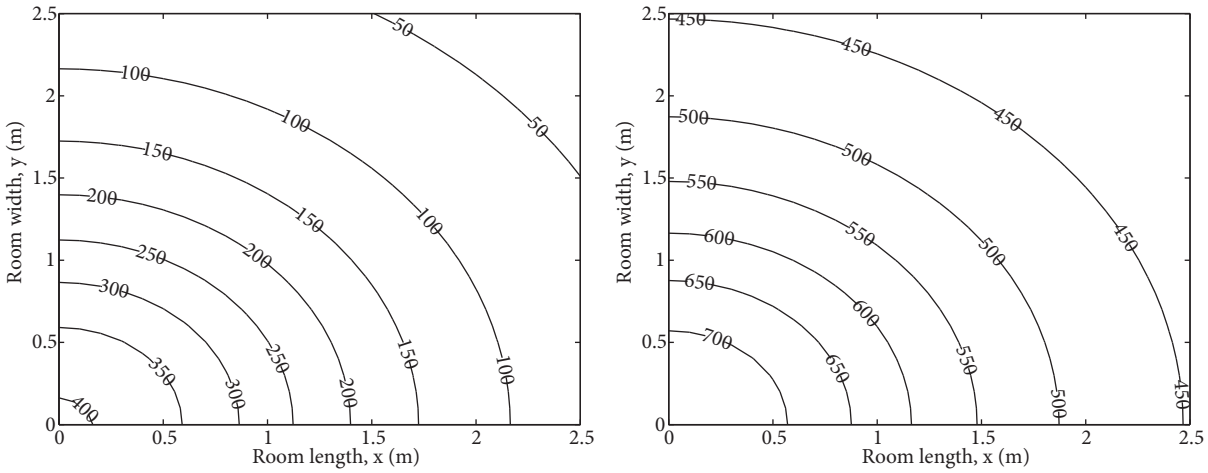


(a) min. 29 lx, mean 147 lx, max. 404 lx

(b) min. 408 lx, mean 514 lx, max. 746 lx

**Figure 5**. Horizontal brightness distribution in lx for (a) reference channel and (b) repeater-assisted channel.

### 4.3. SNR improvement vs. the receiver location

Figures 6a and 6b show the actual SNR distribution inside the room on the desktop surface. The SNR is derived by using Eq. (11) over 2 MHz bandwidth and the data rate $R_b$ of 1 Mbps. In the reference channel model,

the average SNR is 16.30 dB, whereas the SNR is increased to 19.49 dB in the repeater-assisted model. The BER for 2-PPM is $Q(\sqrt{SNR})$ [10]. In order to achieve BER $P_e$ of $10^{-3}$, the required SNR is 9.8 dB and, similarly for $P_e$ of $10^{-6}$, the required SNR is 13.5 dB. Therefore, the transmission rate of 1 Mbps is achievable in both reference channel and the channel with the repeater. The normalized area with SNR $>$ 13.5 dB for the reference channel is 70%, whereas the normalized area for the same SNR constraint is enhanced to 90% with the repeater-assisted channel. Higher data rates are not allowed due to the modulation bandwidth of the white LEDs. The SNR values presented here are subject to change depending on the shot noise, which is associated with the background light-induced current. For instance, when the receiver is exposed to direct sunlight, the SNR may decrease.

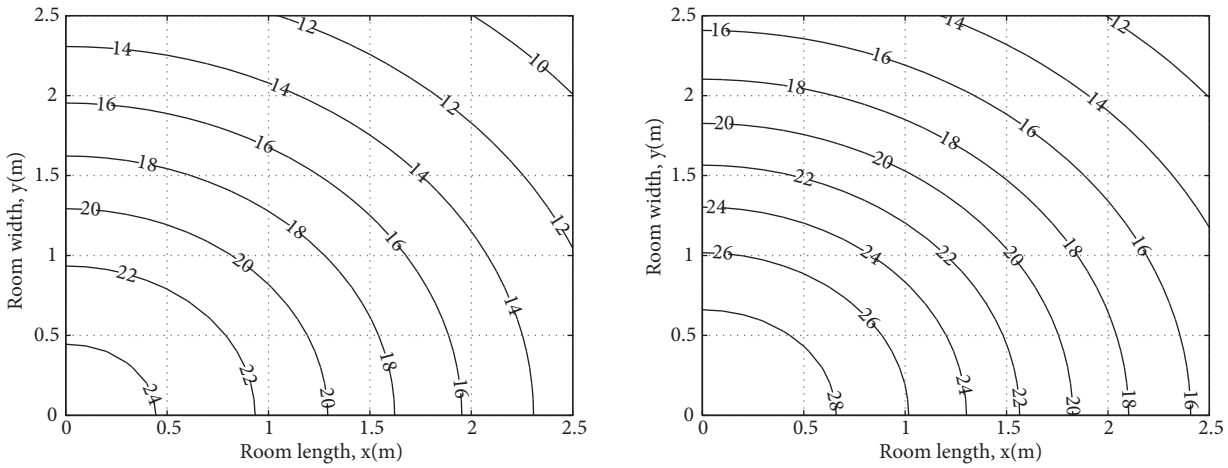


**Figure 6**. Distribution of the SNR (dB): (a) reference channel and (b) repeater-assisted channel.

Figure 7a gives the distribution of SNR improvement achieved with the repeater in the room area. Here, again the improvement in SNR is defined as the SNR gain achieved by the repeater with respect to the reference model when the BER is $10^{-3}$. The improvement in SNR increases when the receiver gets closer to the center of the room. This is mainly because of the shortened distances for the source-repeater and the source-destination links, which accordingly increase in the total received power. When the receiver is at location (1,1), the SNR improvement with respect to the reference channel is 3.8 dB. Similarly, when the receiver is at (1.5,1.5) and (2,2), the SNR gains become 3 dB and 2.30 dB, respectively.

Figure 7b displays the BER versus $E_b/N_0$ for the reference channel (solid lines) and for the channel with the repeater (dotted lines). Computer simulation results are also indicated (stars). $E_b/N_0$ is given with respect to the reference channel where no repeating takes place. The SNR improvement results in Figure 7a can also be observed in Figure 7b.

### 4.4. Effect of shadowing

When the room is empty and the LOS link is not shadowed, the channel with the repeater outperforms the reference model (average SNR improvement of 2.78 dB when BER $= 10^{-3}$). When the LOS path of the source-destination link is obstructed due to the moving objects of people in the room, the data are transmitted over the diffused portion of that channel. Figure 8a gives the BER performance improvement with the repeater when the LOS component for the source-destination link is obstructed in 1% of time. When the receiver is at location (1,1), the SNR gain is 4.7 dB, whereas in the unshadowed environment the gain is 3.8 dB for the same

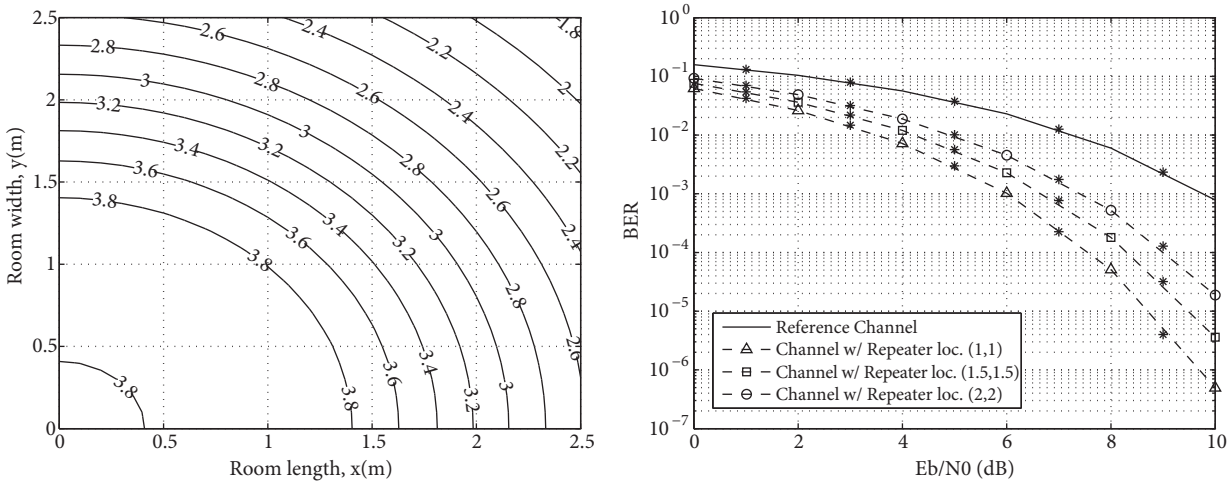


(a) SNR improvement distribution for BER = $10^{-3}$.

(b) BER vs. $E_b/N_0$ for the reference channel and the channel with a repeater.

**Figure 7**. SNR improvement and the BER results for the channel with repeater.

set up, as shown in Figure 7b. Similarly, the SNR gains for locations (1.5,1.5) and (2,2) are 3.5 dB and 2.6 dB, respectively. When the chance of shadowing is increased, the impact of the repeater on the BER performance is more distinct. Figure 8b displays the BER curves for the blocking probability of 10%. In this case, the SNR gains are 7.75 dB, 5.5 dB, and 3.5 dB for the receiver locations of (1,1), (1.5,1.5), and (2,2), respectively.

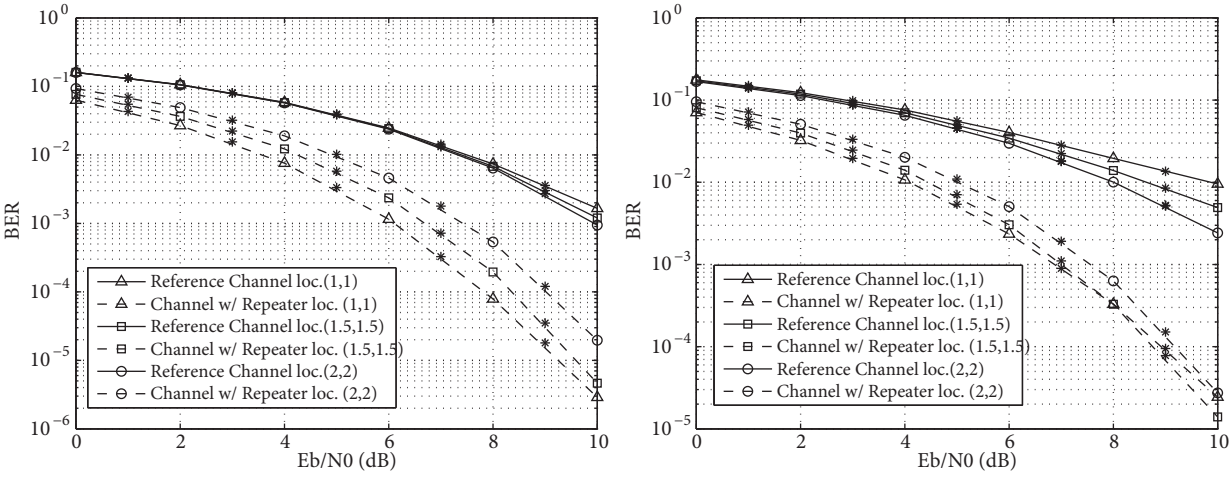


(a) 1% shadowing

(b) 10% shadowing

**Figure 8**. BER performance improvement with the repeater when the channel is shadowed.

## 5. Conclusion

In conclusion, visible light communication has been recently proposed as an alternative way of data transmission. Future lighting systems will be composed of white LEDs and there might be more than one light source in the environment. In this study, we have considered a second light source, which is mounted at a desk as a repeater terminal. We have shown that the repeater-assisted VLC network outperforms conventional VLC networks in terms of both reliability and illuminance. The considered VLC repeater can be employed in any VLC system without any prior work.

The visible light channel without any intermediate terminal can provide 90 MHz bandwidth for a typical office environment. When a repeater is included, the bandwidth efficiency of the system is reduced, and the channel bandwidth becomes 3–5 MHz due to the extent of the time dispersion in the channel. In this work, the bandwidth of the transmission has been set to the modulation bandwidth of the white LEDs, 2 MHz. Both the reference channel and the channel with a repeater can support 2 MHz bandwidth. We have set the transmission data rate to 1 Mbps and considered the 2-PPM modulation scheme. We have investigated power efficiency of the system with the repeater. The average SNR gain for BER of $10^{-3}$ with the repeater in an unshadowed environment is found to be 2.78 dB, whereas when the receiver is shadowed, the increase in SNR is more significant and can be up to 7.75 dB.

In this work, we have considered 2-PPM as the modulation scheme; however, the results can be extended for other modulation schemes. The power allocation between different light sources is potentially the most beneficial direction for future research.

## References


[1] H.B.C. Wook, T. Komine, S. Haruyama, M. Nakagawa, "Visible light communication with LED-based traffic lights using 2-dimensional image sensor", IEEE Consumer Communications and Networking Conference, Vol. 1, pp. 243–247, 2006.

[2] G. Pang, T. Kwan, H. Liu, C.H. Chan, "A novel use of LEDs to transmit audio and digital signals", IEEE Industry Applications Magazine, Vol. 8, pp. 21–28, 2002.

[3] Y. Ito, S. Haruyama, M. Nakagawa, "Rate-adaptive transmission on a wavelength dependent channel for underwater wireless communication using visible light LEDs", IEIC Technical Report, Vol. 105, pp. 127–132, 2006.

[4] K. Lee, H. Park, "Modulations for visible light communications with dimming control", IEEE Photonics Letters, Vol. 23, pp. 1136–1138, 2011.

[5] I.E. Lee, M.L. Sim, F.W.L Kung, "Performance enhancement of outdoor visible-light communication system using selective combining receiver", IET Optoelectronics, Vol. 3, pp. 30–39, 2009.

[6] S. Kaur, W. Liu, D. Castor, VLC Dimming Proposal, IEEE Project 802.15-15-09-0641-00-0007, New York, 2009.

[7] M. Safari, M. Uysal, "Relay-assisted free-space optical communication", IEEE Transactions on Wireless Communications, Vol. 7, pp. 5441–5449, 2008.

[8] M. Karimi, M. Nasiri-Kenari, "Free space optical communications via optical amplify-and-forward relaying", Journal of Lightwave Technology, Vol. 29, pp. 242–248, 2011.

[9] M. Karimi, M. Nasiri-Kenari, "BER analysis of cooperative systems in free-space optical networks", Journal of Lightwave Technology, Vol. 27, pp. 5639–5647, 2009.

[10] J.G. Proakis, M. Salehi, Communication Systems Engineering", 2nd ed., Upper Saddle River, NJ, USA, Prentice Hall, 2002.

[11] G. Corbellini, S. Schmid, S. Mangold, T.R. Gross, A. Mkrtchyan, "LED-to-LED visible light communication for mobile applications", in Demo at ACM SIGGRAPH 2012, available at http://people.inf.ethz.ch/schmist/papers/Siggraph2012DemoVLC.pdf.

[12] T. Komine, M. Nakagawa, "Integrated system of white LED visible light communication and power line communication", IEEE Transactions on Consumer Electronics, Vol. 49, pp.1762–1766, 2003.

[13] J. Boyer, D.D. Falconer, H. Yanikomeroglu, "Multihop diversity in wireless relaying channels", IEEE Transactions on Communications, Vol. 52, pp. 1820–1830, 2004.

[14] S. Jivkova, M. Kavehrad, "Shadowing and blockage in indoor optical wireless communications", in IEEE Global Telecommunications Conference, Vol. 6, pp. 3269–3273, 2003.

[15] T. Komine, M. Nakagawa, "A study of shadowing on indoor visible-light wireless communication utilizing plural white LED lightings", in Symposium on Wireless Communications Systems, pp. 36–40, 2004.

[16] J. Grubor, S. Randel, K.D. Langer, J.W. Walewski, "Broadband information broadcasting using LED-based interior lighting", Journal of Lightwave Technology, Vol. 26, pp. 3883–3892, 2008.

[17] Z. Ghassemlooy, W. Popoola, S. Rajbhandari, Optical Wireless Communications: System and Channel Modelling with MATLAB, Boca Raton, FL, USA, CRC Press, 2012.

[18] J.R. Barry, Wireless Infrared Communication, Boston, Kluwer, 1994.

[19] J.M. Kahn, W.J. Krause, J.B. Carruthers, "Experimental characterization of non-directed indoor infrared channels", IEEE Transactions on Communications, Vol. 43, pp. 1613–1623, 1995.

[20] J.R. Barry, J.M. Kahn, W.J. Krause, E.A. Lee, D.G. Messerschmitt, "Simulation of multipath impulse response for indoor wireless optical channels", IEEE Journal on Selected Areas in Communications, Vol. 11, pp. 367–379, 1993.

[21] V. Jungnickel, V. Pohl, S. Nonnig, C. von Helmolt, "A physical model of the wireless infrared communication channel", IEEE Journal on Selected Areas in Communications, Vol. 20, pp. 631–640, 2002.

[22] J.M. Kahn, J.R. Barry, "Wireless infrared communications", Proceedings of IEEE, Vol. 85, pp. 265–298, 1997.

[23] K. Lee, H. Park, J.R. Barry, "Indoor channel characteristics for visible light communications", IEEE Communications Letters, Vol. 15, pp. 217–219, 2011.

[24] T. Komine, M. Nakagawa, "Fundamental analysis for visible-light communication system using LED lightings", IEEE Transactions on on Consumer Electronics, Vol. 50, pp. 100–107, 2004.

[25] R.U. Nabar, H. Boelcskei, F.W. Knueubhueler, "Fading relay channels: performance limits and space-time signal design", IEEE Journal on Selected Areas in Communications, Vol. 22, pp. 1099–1100, 2000.

[26] Z. Ghassemlooy, A.R. Hayes, B. Wilson, "Reducing the effects of intersymbol interference in diffuse DPIM optical wireless communication", IEE Proceedings on Optoelectronics, Vol. 150, pp. 445–452, 2003.

[27] K.K Wong, T. OFarrell, M. Kiatweerasakul, "Infrared wireless communications using spread spectrum techniques", IEE Proceedings on Optoelectronics, Vol. 147, pp. 308–314, 2000.

[28] J.B. Carruthers, J.M. Kahn, "Angle diversity for nondirected wireless infrared communication", IEEE Transactions on Communications, Vol. 48, pp. 960–969, 2000.

[29] T. Komine, L.J. Hwan, S. Haruyama, M. Nakagawa, "Adaptive equalization for indoor visible-light wireless communication systems", Asia-Pacific Conference on Communications, pp. 294–298, 2005.

[30] Texas Instruments,"LM359 Dual, High Speed, Programmable, Current Mode (Norton) Amplifiers", Texas Instruments, May 2004. 2004.